Cosmic Acceleration from a Two-Component Dark Matter Superfluid

Alexander Ziegenhorn

Thesis submitted for the degree of
Master of Science in Astronomy

Institute of Theoretical Astrophysics
University of Oslo

November 6, 2020

Abstract

We investigate the cosmological implications of a two-component dark matter superfluid as proposed by Ferreira et al. (2019). Through contact interactions between the axion-like particles in these components, a late-time potential dominates the energy content of the universe and leads to vacuum energy-like accelerated expansion. We test this model in three ways: by evolving the Hubble parameter to very late-times, by comparing the luminosity distance to type 1a supernova observations, and by comparing theoretical values of the CMB shift parameter and dark matter density parameter to those from WMAP.

In terms of the Hubble parameter, we find that it is similar to ΛCDM from the surface of last scattering until the present when the interaction potential causes a significant difference. We find that the luminosity distances predicted by the model agree with supernova distance moduli for $z < 1.3$ for a certain range of energy gaps between the two superfluid states. Finally, given accepted CMB shift parameter values, we derive constraints on the dark matter density parameter $\Omega_m = .255 \pm .035$, which agrees with that from SDSS-II/SNLS results of $\Omega_m = .295 \pm .035$.

Acknowledgments

I first want to thank my advisor Øystein Elgarøy for his supervision and guidance of my thesis: your patience and wisdom inspire me to grow as a scientist and solve problems I never thought possible.

I also want to thank my family for their unending love and support throughout my studies: your encouragement of me to pursue my dreams means the universe to me.

I also appreciate Øyvind Christiansen's effort in proofreading this thesis, as well as all the fruitful discussions we've had and of course all the chess we played.

Lastly, I want to recognize my friends at the Stellar Cellar: moving to a new country to study astrophysics is by no means easy, but your support allowed me to do just that. Thanks for all the memories I've made here og tusen takk for at dere hjalp meg med å lære norsk!

Contents

Chapter 1

Introduction

The *Lambda Cold Dark Matter* (ΛCDM) model is currently regarded as the standard cosmological paradigm: it describes the evolution, matter content, and large-scale structure of the Universe with remarkable accuracy [1]. It posits that the accelerated expansion of the universe is caused by some *dark energy* that acts like a cosmological constant (hence Λ), as well as the existence of a cold (i.e. non-relativistic), pressureless fluid of weakly interacting particles, termed *dark matter* (hence *CDM*), whose existence has robust indirect observational evidence [2].

ΛCDM is not without its deficiencies, however. The Standard Model of particle physics does not predict the existence of anything akin to dark matter and any direct detection or production remains elusive. There are also several notable small-scale problems with ΛCDM that have been observed, including: the *Baryonic Tully-Fisher relation* [3], the *"Too Big to Fail" problem* [4], and the *cusp/core problem* [5] (see [6] for a list of several others). If dark energy is truly described by a cosmological constant, then there is a discrepancy between the value as deduced from cosmology and that predicted by quantum field theory (which by some estimates differs by 120 orders of magnitude), leading to the *cosmological constant problem* [7].

In an attempt to remedy discrepancies on small-scales, Milgrom (1983) [8] proposed replacing particle dark matter with modified Newtonian dynamics (MOND) on galactic scales, such that gravitational acceleration differs from Newtonian predictions. Its successes are apparent in its agreement with the Baryonic Tully-Fisher Relation and flat galactic rotation curves. MOND is not effective however on galactic cluster-scales, where the dynamics can again be described by ΛCDM.

This motivates the introduction of a new model that includes the successes of ΛCDM on large scales while also preserving MOND on galactic scales. Recent publications attempting to unify the two have utilized a theory of superfluid dark matter. Ferreira et al. (2019) in [9] developed a theory of superfluid dark matter (hereafter the *Berezhiani-Ferreira-Khoury* or *BFK* model) that is able to explain the evolution of the Universe

through the matter dominated epoch to the present, while also accounting for late-time cosmic acceleration. They posit that dark energy is the potential resulting from the interaction between two Bose-Einstein condensed dark matter states in galactic halos. This model effectively unifies the dark sector while also accounting for ΛCDM observations and MONDian effects.

This thesis is organized as thus: an introduction to the theory of accelerated expansion resulting from popular (but ultimately insufficient) theories, namely, the cosmological constant, quintessence, and (briefly) modified gravity (Chapter 2); Chapter 3 provides an overview of Bose-Einstein condensates and their connection to superfluidity in the languages of statistical mechanics and field theory/symmetries; with these two chapters, we are able to discuss the BFK model in-depth both qualitatively and quantitatively in Chapter 4; and finally in Chapter 5 we perform cosmological and numerical tests on the BFK model and compare the results to those from ΛCDM.

Therefore, the goal of this work is three-fold: to provide a comprehensive introduction to dark matter in a superfluid state and its connection to late-time accelerated expansion, to elucidate the intermediary steps in Ferreira et al.'s derivations and qualitative descriptions, and to test their model with observational data.

A Note on Notation

One should make note of the conventions used throughout this work: we use *natural units* where $c = \hbar = k_B = 1$, and the metric signature $(-,\ +,\ +,\ +)$. Greek indices run from zero to three and represent spacetime coordinates, while Latin indices go from one to three and generally represent spatial coordinates; Einstein summation notation is implied for repeated indices. We assume a spatially-flat universe (i.e. there is no curvature).

All code for this project can be found at: [GitHub].

Chapter 2

The Dark Energy Problem

Evidence for the accelerated expansion of the Universe is abundant (as evident in supernova observations [10], for example), yet the underlying mechanism remains elusive. There are two ways in which one may mathematically account for this: given Einstein's field equations, either modify the energy content of the universe to include a dark energy component - popular choices include a cosmological constant and quintessence (among *many* others) - or modify the dynamics of spacetime as in modified gravity theories (c.f. $f(R)$). This chapter discusses the aforementioned examples with a particular emphasis on dark energy models.

2.1 The Cosmological Constant

Although originally introduced by Einstein to describe his static universe model, the inclusion of a constant Λ (the *cosmological constant*) to the field equations is one way to produce accelerated expansion in a universe. The Einstein field equations are thus

$$G_{\mu\nu} + \Lambda g_{\mu\nu} = 8\pi G T_{\mu\nu}. \tag{2.1}$$

Here $G_{\mu\nu}$ is the Einstein tensor while G is the Newtonian gravitational constant. If we assume that Λ contributes to the total energy density of the universe, then we should find its contribution to the energy-momentum tensor $T_{\mu\nu}$. To do this, we first introduce the notion of the line element: how distance is measured in spacetime

$$ds^2 = g_{\mu\nu} dx^\mu dx^\nu. \tag{2.2}$$

This says that the infinitesimal distance ds^2 between two events with coordinate distance dx^μ is given by the metric tensor.

By assuming the universe is expanding, homogeneous, and isotropic,[†] we can express

[†] Assuming a *homogeneous* and *isotropic* universe is known as the *cosmological principle*. Homogeneity assumes that on sufficiently large scales, matter is evenly distributed. Isotropy is defined such that a freely-falling observer (one that moves with the average velocity of local galaxies) measures little to no variation in radiation in any direction.

the line element with the Friedmann-Lemaître-Robertson-Walker (FRLW) metric

$$ds^2 = -dt^2 + a^2(t)\delta_{ij}dx^i dx^j \tag{2.3}$$

(δ_{ij} is the Kronecker) so that the metric tensor is

$$g_{\mu\nu} = \begin{pmatrix} -1 & 0 & 0 & 0 \\ 0 & a^2 & 0 & 0 \\ 0 & 0 & a^2 & 0 \\ 0 & 0 & 0 & a^2 \end{pmatrix}. \tag{2.4}$$

We choose to describe the matter content as a perfect fluid[‡]

$$T^{\mu\nu} = (\rho + p)U^\mu U^\nu + pg^{\mu\nu} \tag{2.5}$$

$$T^{\mu\nu} = \begin{pmatrix} \rho & 0 & 0 & 0 \\ 0 & p/a^2 & 0 & 0 \\ 0 & 0 & p/a^2 & 0 \\ 0 & 0 & 0 & p/a^2 \end{pmatrix} \tag{2.6}$$

such that (2.6) is in the frame of an observer locally co-moving with the fluid. The conservation of $T^{\mu\nu}$ is given by

$$\nabla_\mu T^{\mu 0} = \partial_\mu T^{\mu 0} + \Gamma^\mu_{\mu\sigma} T^{\sigma 0} + \Gamma^0_{\mu\sigma} T^{\mu\sigma} = 0 \tag{2.7}$$

$$= \dot{\rho} + 3\frac{\dot{a}}{a}(\rho + p). \tag{2.8}$$

This is solved using an equation of state

$$p = w\rho \tag{2.9}$$

so that the solution to (2.8) goes as

$$\rho \propto a^{-3(1+w)}. \tag{2.10}$$

From the second Friedmann equation [11]

$$\frac{\ddot{a}}{a} = \frac{-4\pi G}{3}(\rho + 3p) \tag{2.11}$$

the condition for acceleration is $\ddot{a} > 0$, which implies

$$\rho + 3p < 0. \tag{2.12}$$

A reasonable assumption is to only consider dark matter ($p_m = 0$) and dark energy

$$\rho_m + \rho_\Lambda + 3p_\Lambda < 0 \tag{2.13}$$

[‡] p, ρ, and U^μ are the pressure, density, and four-velocity of the fluid respectively.

but at late times $\rho_m \ll \rho_\Lambda$

$$\begin{aligned} \rho_\Lambda + 3p_\Lambda &< 0 \\ (1+3w_\Lambda)\rho_\Lambda &< 0 \\ \Rightarrow w_\Lambda &< -\frac{1}{3} \end{aligned} \tag{2.14}$$

where in the second line we used the relation (2.9). Therefore, in order to have an accelerating universe, the equation of state parameter for dark energy should be less than negative one third. A natural physical interpretation for the cosmological constant is the vacuum energy contributions from all Standard Model fields. In quantum field theory, the vacuum state[§] of a quantum field is the field's lowest energy state in which no particles inhabit, but is not necessarily zero, either. In general relativity though, all energy gravitates, so these zero-point energies should be included in $T_{\mu\nu}$. If we are indeed considering a vacuum energy, then we must ensure that it is Lorentz invariant. By requiring this, we find that $w = -1$ implying

$$p = -\rho \tag{2.15}$$

because the energy density must be homogeneous [12]. Now by substituting (2.15) into (2.5), we get the energy-momentum tensor for Λ

$$T_{\mu\nu,\Lambda} = \rho_\Lambda g_{\mu\nu} \tag{2.16}$$

and by introducing this into the Einstein field equations

$$\begin{aligned} R_{\mu\nu} - \frac{1}{2}Rg_{\mu\nu} + \Lambda g_{\mu\nu} &= 8\pi G T^{matter}_{\mu\nu} + 8\pi G \rho_\Lambda g_{\mu\nu} \\ \Rightarrow \rho_\Lambda &= \frac{\Lambda}{8\pi G}. \end{aligned} \tag{2.17}$$

We also find that the scale factor evolves as $a \propto e^{H_0 t}$ (compare to $a_\gamma \propto t^{1/2}$ and $a_m \propto t^{2/3}$, the scale factors of radiation and matter, respectively).

Why does it not work?

The most pressing issue with having a cosmological constant that acts like vacuum energy is an enormous discrepancy between the energy density of the vacuum energy implied from observation and that from theory. We quote values from [13] for convenience. Energy density is equivalent to a quartic mass scale: $\rho_\Lambda = M^4_{vac}$. One expects the ratio of the theoretical value to the observed value to be of the order 1, but instead

$$\frac{M_{\text{vac, theory}}}{M_{\text{vac, obs}}} = \frac{M_{Planck}}{M_{\text{vac, obs}}} \sim \frac{10^{18}\text{GeV}}{10^{-12}\text{GeV}} \sim 10^{30}. \tag{2.18}$$

[§]Also known as the *zero-point energy*.

The origin of the oft-quoted $\mathcal{O}(120)$-discrepancy come from raising this to the fourth power (in reference to the energy density), but $\mathcal{O}(30)$ is a bit more "fair". Nevertheless, a discrepancy of thirty orders of magnitude is hard (if not impossible) to rectify and is the source of the cosmological constant problem. The answer as to why the cosmological constant is so small compared to predictions from the Standard Model is an elusive and long-standing problem, naturally leading researching to look elsewhere for an explanation of dark energy. Arguably the simplest alternative is a light scalar field dubbed quintessence. Using a scalar field to explain dark energy phenomena does not necessarily preclude a non-zero vacuum energy, but generally in alternatives to the cosmological constant, $\Lambda = 0$. This is because the observed energy density is already incredibly small and evidently the Standard Model zero-point energies do not contribute as expected. Also by assuming $\Lambda = 0$, analysis is simplified: attempting to attribute observations to two different sources could result in degeneracies and it would likely be difficult (impossible) to attribute individual contributions.

2.2 Quintessence

Quintessence models of dark energy are characterized as scalar fields minimally coupled to gravity with a time-dependent equation of state. One find that certain potentials cause late-time accelerated expansion. Let us then consider the action $S[\Phi,\ g_{\mu\nu}]$ of a homogeneous, real, scalar field $\Phi(t)$ in a gravitational field with metric $g_{\mu\nu}$ and vary it with respect to the metric

$$S[\Phi(t),\ g_{\mu\nu}] = S_{gravity}[g_{\mu\nu}(x^\beta)] + S_{matter}[\Phi(t),\ g_{\mu\nu}]. \tag{2.19}$$

The equations of motion follow from the principle of least action

$$\frac{\delta S}{\delta g^{\mu\nu}} = \frac{\delta S_{gravity}}{\delta g^{\mu\nu}} + \frac{\delta S_{matter}}{\delta g^{\mu\nu}} = 0. \tag{2.20}$$

From the action, we can derive an expression for the energy-momentum tensor of the field. This in turn gives expressions for the density and pressure associated with the field. These two quantities are then used in the calculation of the equation of state and this is compared to the equation of state for the cosmological constant. The energy-momentum tensor for the scalar field

$$\begin{gathered} T_{\mu\nu} \sim \frac{\delta S_{matter}}{\delta g^{\mu\nu}} \\ T_{\mu\nu}\ \delta g^{\mu\nu} \sim \delta S_{matter} \\ T_{\mu\nu}\ \delta g^{\mu\nu} \sim \delta \int d^4x \sqrt{-g} \left(-\frac{1}{2} g^{\sigma\gamma} \partial_\sigma \Phi \partial_\gamma \Phi - V(\Phi) \right) \\ = \int d^4x \left\{ \delta \left(\sqrt{-g} \right) \left(-\frac{1}{2} g^{\sigma\gamma} \partial_\sigma \Phi \partial_\gamma \Phi - V(\Phi) \right) + \sqrt{-g}\ \delta \left(-\frac{1}{2} g^{\sigma\gamma} \partial_\sigma \Phi \partial_\gamma \Phi - V(\Phi) \right) \right\}. \end{gathered} \tag{2.21}$$

A useful identity helps us progress [14]

$$\delta\sqrt{-g} = -\frac{1}{2}\sqrt{-g}\; g_{\mu\nu}\delta g^{\mu\nu}\,: \tag{2.22}$$

$$\begin{aligned} T_{\mu\nu}\;\delta g^{\mu\nu} \sim \int d^4x \Bigg\{ -\frac{1}{2}\sqrt{-g} g_{\mu\nu}\delta g^{\mu\nu} \left(-\frac{1}{2}g^{\sigma\gamma}\partial_\sigma\Phi\partial_\gamma\Phi - V(\Phi)\right) \\ + \sqrt{-g}\left(-\frac{1}{2}\delta g^{\sigma\gamma}\partial_\sigma\Phi\partial_\gamma\Phi\right)\Bigg\} \\ = -\frac{1}{2}\int \sqrt{-g}d^4x \Bigg\{ \underbrace{\partial_\mu\Phi\partial_\nu\Phi + g_{\mu\nu}\left(-\frac{1}{2}g^{\sigma\gamma}\partial_\sigma\Phi\partial_\gamma\Phi - V(\Phi)\right)}_{T_{\mu\nu}} \Bigg\}\delta g^{\mu\nu}. \end{aligned}$$

Then by identifying a factor of $-2/\sqrt{-g}$

$$\Rightarrow T_{\mu\nu} \equiv \frac{-2}{\sqrt{-g}}\frac{\delta}{\delta g^{\mu\nu}}S_{matter}. \tag{2.23}$$

The density and pressure of the field are found from the trace of the energy-momentum tensor $T^\mu_{\ \nu} = \mathrm{diag}(-\rho,\ p,\ p,\ p)$

$$\begin{aligned} g^{\mu\alpha}T_{\alpha\nu} = T^\mu_{\ \nu} &= g^{\mu\alpha}\partial_\alpha\Phi\partial_\nu\Phi + g^{\mu\alpha}g_{\alpha\nu}\left(-\frac{1}{2}g^{\sigma\gamma}\partial_\sigma\Phi\partial_\gamma\Phi - V(\Phi)\right) \\ \rho = -T^0_{\ 0} &= -\left\{\partial^0\Phi\partial_0\Phi + \delta^0_0\left(-\frac{1}{2}g^{\sigma\gamma}\partial_\sigma\Phi\partial_\gamma\Phi - V(\Phi)\right)\right\} \\ &= -\left\{-\partial^0\Phi\partial_0\Phi + \left(-\frac{1}{2}\left(-\partial^0\Phi\partial_0\Phi + \partial^i\Phi\partial_i\Phi\right) - V(\Phi)\right)\right\} \\ &= \dot\Phi^2 - \left(\frac{1}{2}\dot\Phi^2 - \frac{1}{2}\left(\nabla\Phi\right)^2 - V(\Phi)\right) \\ &= \boxed{\frac{1}{2}\dot\Phi^2 + V(\Phi)}; \end{aligned} \tag{2.24}$$

$$\begin{aligned} p = T^i_{\ i} &= \partial^i\Phi\partial_i\Phi + \delta^i_i\left(-\frac{1}{2}g^{\sigma\gamma}\partial_\sigma\Phi\partial_\gamma\Phi - V(\Phi)\right) \\ &= (\nabla\Phi)^2 + \left(\frac{1}{2}\dot\Phi^2 - (\nabla\Phi)^2 - V(\Phi)\right) \\ &= \boxed{\frac{1}{2}\dot\Phi^2 - V(\Phi)}. \end{aligned} \tag{2.25}$$

Using the definition for the equation of state w (2.9) as before

$$\begin{aligned} w &= \frac{p}{\rho} \\ &= \frac{\frac{1}{2}\dot\Phi^2 - V(\Phi)}{\frac{1}{2}\dot\Phi^2 + V(\Phi)}. \end{aligned} \tag{2.26}$$

Reference back to the second Friedmann equation and substitute in our expressions for ρ and p

$$\begin{aligned}\frac{\ddot{a}}{a} &= \frac{-4\pi G}{3}\left[\rho + 3p\right] \\ &= \frac{-4\pi G}{3}\left[\frac{1}{2}\dot{\Phi}^2 + V(\Phi) + 3\left(\frac{1}{2}\dot{\Phi}^2 - V(\Phi)\right)\right] \\ &= \frac{-8\pi G}{3}\left[\dot{\Phi}^2 - V(\Phi)\right]; \end{aligned} \tag{2.27}$$

thus $\ddot{a}/a > 0$ only when $V(\Phi) > \dot{\Phi}^2$. If we assume the field is slowly rolling (i.e. $V(\Phi) \gg \dot{\Phi}^2$), then we recover the equation of state for the cosmological constant

$$w \approx \frac{-V(\Phi)}{V(\Phi)} \approx -1. \tag{2.28}$$

What is wrong with quintessence?

Currently no scalar field similar to quintessence is predicted by the Standard Model, forcing one to look at physics beyond the Standard Model. Even then, one is hard-pressed to find a suitable candidate: since the mass of the field is very small, it leads to fine-tuning issues. This follows from the fact that the mass of the quintessence field is proportional to the steepness of its potential: in order to produce an equation of state of -1, the mass must be very small.

2.3 Alternative Theories of Gravity

The mathematics portion of this section follows a review of $f(R)$ theories in [15]. As opposed to modifying the matter-energy content of the universe (such as in models of quintessence), alternative gravity theories (usually *modified gravity*) modify the geometric side ($R_{\mu\nu} - \frac{1}{2}Rg_{\mu\nu}$) of Einstein's equations. Proponents of modified gravity theories may argue that our current description of gravity insufficiently describes gravitational dynamics and leads to phenomena currently labeled as "the dark sector". That is extensions to gravity can account for dark matter and dark energy. A useful toy model in this case is a scalar *f(R) theory* where the Ricci scalar R in the Einstein-Hilbert action

$$S = \frac{1}{16\pi G}\int d^4x\sqrt{-g}R$$

is replaced by a function of R

$$S = \frac{1}{16\pi G}\int d^4x\sqrt{-g}f(R). \tag{2.29}$$

Arguably a large problem with modified gravity theories is that aside from a few select $f(R)$, Einstein's equations become extremely difficult to work with and solve. While

mathematical rigor does not itself exclude the idea of modified gravity, one can argue that it seems unnatural to modified spacetime geometry given the extraordinary correspondence between general relativity and observational evidence. Whatever the case, this thesis is primary concerned with particle dark matter, so we will leave the above as simply another avenue down which one can arrive at dark energy phenomena.

This chapter served as an introduction to the idea of dark energy and why past models are physically insufficient. There are of course more models of dark energy than can be mentioned here, but it suffices to say that this abundance alone points to the general disarray and disagreement in dark energy research. As stated in the introduction, we will cast yet another model for dark matter/dark energy into the foray in the form of superfluid dark matter. Therefore in the following chapter we introduce the concept of Bose-Einstein condensates and superfluidity in preparation for discussing the model at hand.

Chapter 3

Bose-Einstein Condensation and Superfluidity

In this chapter we define Bose-Einstein condensates (BEC) and the effects that allow for their formation - specifically the critical temperature, the thermal de Broglie wavelength, and Bose-Einstein statistics. From this we can discuss superfluids and their dynamics, along with the relation between (broken) symmetries and BEC. The principles covered in this section will later be applied to the dark matter model at hand and its associated properties and dynamics.

3.1 Condensate Theory

3.1.1 Introduction to Condensates

Let us consider a homogeneous, neutral, gas of bosons (integer-spin particles). We remind ourselves that fermions constitute atoms, and since we are examining neutral atoms, the number of protons and electrons must be equal. Thus the specie of an atom is determined by the number of neutrons: an even number of which describes a boson, while an odd number describes a fermion.

As an example, consider neutral rubidium-87, a popular vapor in BEC experiments (not least because it was the first dilute gas to be condensed [16]): it has atomic number 37. Being electrically neutral, it has an equal number of protons and electrons, and fifty neutrons, making it a boson. Some other vapors that have been successfully condensed include lithium-7, potassium-41, and cesium-133. Helium-4 has also been condensed, but it is a special case because its self-interactions are sufficiently strong to form a liquid. Aside from atoms, examples of bosons include mesons (pions, kaons, ...) and the gauge bosons (photons, gluons, and $W^{\pm}/Z^{0}$).

A property unique to bosons is their ability to have multiple particles occupying the

same energy state. Boson wave functions are symmetric under particle exchange

$$\psi(x_1,\ x_2) = +\psi(x_2,\ x_1). \tag{3.1}$$

where x_1 and x_2 are simply labels containing all the information specifying a unique single particle state. Therefore, they are not governed by the Pauli-exclusion principle (unlike fermions) allowing an arbitrary number of them to occupy the same particle state. In this chapter, we are interested in systems where most of the particles are in the lowest energy state.

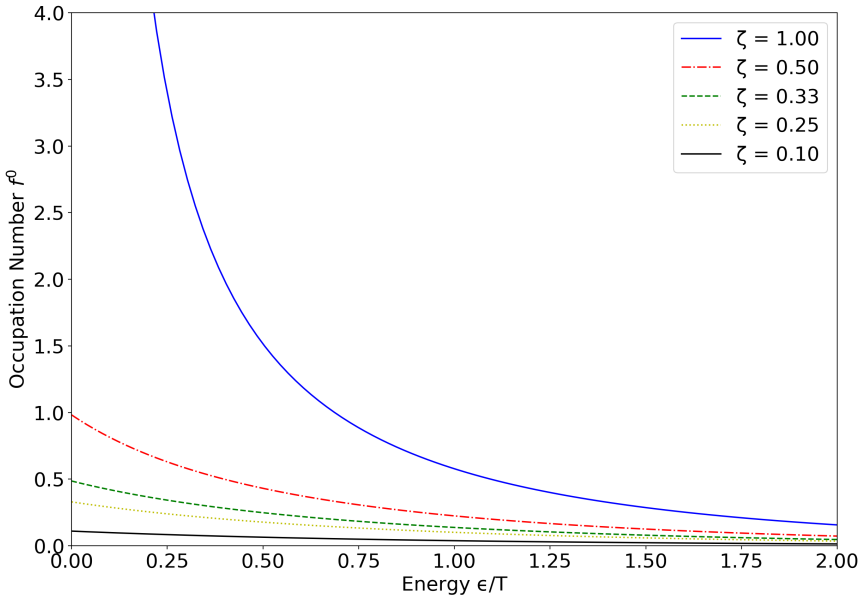

Figure 3.1: The Bose Distribution for various fugacities. $\zeta = 1$ corresponds to Bose-Einstein condensation.

3.1.2 Bose-Einstein Statistics

Bosons are described by Bose-Einstein statistics. Consider the Bose-Einstein distribution function

$$f^0(\epsilon_\nu) = \frac{1}{e^{(\epsilon_\nu - \mu)/T} - 1}. \tag{3.2}$$

This gives the expected number of particles in some state ν for an energy ϵ. $\mu(T,\ V,\ N)$ is the chemical potential, T is temperature, V is volume, and N is the total number of particles. The physical definition of μ is somewhat contested in condensed matter literature, but for our sake we define it as the change in energy by the addition of one

particle to the system (See [17] for other definitions and analysis). If we define the *fugacity* as

$$\zeta \equiv \exp(\mu/T) \tag{3.3}$$

then

$$f(\epsilon/T) = \frac{1}{\zeta^{-1}e^{\epsilon/T} - 1}. \tag{3.4}$$

This allows us to consider f as a function of energy states ϵ/T. f is plotted for various values of ζ in Figure 3.1. The figure shows that by following an isothermal curve one is able to identify the expected number of particles $f(\epsilon/T)$ in each energy state ϵ/T. Notice, when $\zeta = 1$, that the occupation number of the lowest energy state ($\epsilon/T = 0$) asymptotically approaches all of the particles in the system - i.e. the state is macroscopically occupied. It is this macroscopic occupation that we define as a Bose-Einstein condensate. Let us also define the temperature at which Bose-Einstein condensate occurs as the *critical temperature* T_c. In the next subsection we discuss the physical processes behind BECs and the role T_c plays.

3.1.3 Mechanisms

In this subsection we consider a Bose gas initially at a high temperature and examine what happens when it is cooled below the critical temperature. Let this Bose gas be dilute, electrically neutral, and non-interacting. We start with the thermal de Broglie wavelength

$$\lambda_T = \sqrt{\frac{2\pi}{mT}}; \tag{3.5}$$

it goes as

$$\lambda_T \propto \frac{1}{T}. \tag{3.6}$$

While the system is at a high temperature, λ_T is small and the gas can be described classically. As the temperature decreases though, λ_T increases, and there will be a temperature at which the wavelength is proportional to the mean interparticle spacing in the gas. At this point the matter waves of the particles will begin to overlap until the system can be described by a single wave function and behaves as a single macroscopic matter wave.

The macroscopic matter wave nature is famously described by the Gross-Pitaevskii equation. In an interacting Bose gas, when the range of the interaction is much less than the mean interparticle spacing, the entire system is described by a non-linear Schrödinger equation

$$i\hbar\frac{\partial\psi(\vec{r},\ t)}{\partial t} = -\frac{1}{2m}\nabla^2\psi(\vec{r},\ t) + V(\vec{r})\psi(\vec{r},\ t) + U_0|\psi(\vec{r},\ t)|^2\psi(\vec{r},\ t) \tag{3.7}$$

where V is an external trapping potential. This also assumes that interactions are infrequent given the dilute number density and the large difference between the interatomic spacing and interaction scales. Therefore, U_0 results from an effective interaction in order to avoid detailed corrections when considering an N-body system. It is of the form

$$U_{\text{eff}}(\vec{r} - \vec{r}') = U_0 \delta(\vec{r} - \vec{r}').$$

Critical Temperature Estimation

This derivation was originally done in [18]. Remarkably, we can estimate the critical temperature for a non-interacting Bose gas using dimensional analysis. We can first derive an energy

$$\varepsilon = \frac{\hbar^2 n^{2/3}}{m}, \tag{3.8}$$

where n is the particle density and m is the particle mass. We find a temperature when dividing by k_B

$$T_c = C\frac{\hbar^2 n^{2/3}}{m k_B}. \tag{3.9}$$

where C is a numerical factor that results when determining the number of particles in excited states at T_c. For our purposes, its origin is not of great important as we just want an order-of-magnitude estimation. By substituting in the values for helium-4, we find a theoretical critical temperature of 3.13K, which is remarkably close to the experimental value of 2.17K [19, 20], especially considering helium-4 is strongly self-interacting, not dilute, and a liquid rather than a gas, at T_c. While this calculation provides agreeable results, it serves to highlight the important role interactions play in BEC and especially in superfluidity - we will expound upon this later.

3.1.4 Some Physical Intuition

One may find it beneficial to consider the physical extents of Bose-Einstein condensed systems. In typical experiments, BEC particle densities range from 10^{13} to 10^{15} particles / cm^3 while that of air is 10^{19} particles / cm^3 [18]. Even though $T_c \sim 1$K, experiments often involve temperatures of the order micro- or nanokelvin, and in the lowest-temperature experiments: picokelvin. Lower temperatures produce purer condensates. BEC matter waves exhibit macroscopic phenomena, meaning they can be visible to the naked eye - a condensate can be about 1mm in size in a laboratory setting [21].

3.2 Superfluidity

We now turn our discussion to one of the most pertinent properties of BEC: *superfluidity*. For a condensate to exhibit superfluidity implies several properties: it flows seemingly

without viscosity (i.e. without energy dissipation) and it has *two* sound speeds. We concentrate on the former.

These phenomena are based off a model of superfluids that requires a so-called *two-fluid* description. We will refer to the two components as the *normal component* and the *superfluid component*. The former refers to the particles in an uncondensed state - that is any particle that has an energy higher than the ground state energy. This component behaves as a classical fluid. Of note, this component includes not only the uncondensed particles, but also the *collective excitations*[†] of the system. Collective excitations are not physical particles, but rather they are mathematical tools created to describe complex dynamics as if the dynamic itself was a particle. This is done in order to simplify analysis. The collective excitation of our interest is the phonon.[‡] Phonons are defined as quantized sound waves (or density perturbations) - sound waves in a quantized system.

The second component, the superfluid component, is therefore the remaining particles in the system - those in the BEC ground state. We say that the normal and superfluid components are indistinguishable and interpenetrating, meaning that one cannot see the difference between the two (there are no physical boundaries between them), as opposed to what one would see with a mixture of two different atoms or molecules.

We remark that all of the entropy in the system is carried by the normal component. Because we are assuming that the condensed particles are in the ground state, the entropy

$$S = \ln \Omega$$

is zero (the number of microstates $\Omega = 1$ since we are only considering particles in one state - the ground state).

3.2.1 The Landau Criterion

This section will discuss the condition that allows a BEC to exhibit superfluidity; this is referred to as the *Landau criterion*. Our definition of a superfluid states that it must flow without viscosity. Therefore, let us find the minimum velocity necessary for an obstacle moving through the condensate to create an excitation in the BEC. When this occurs, the BEC is no longer a superfluid because of energy dissipation.

Consider then a BEC moving through a narrow capillary. Let the reference frame first be in the BEC frame where the fluid is stationary and the capillary is moving to the left with respect to the BEC. An excitation of the superfluid in this frame has energy ϵ_0. By

[†]The term *collective excitation* usually refers to emergent particles in superfluid systems, while *quasi-particles* is usually reserved for *superconducting* systems. But there is no widely agreed upon nomenclature, so one may find the terms are used interchangeably in the literature.

[‡]There exist a plethora of quasi-particles - another that exists in superfluid systems is the roton: the quantum of rotation that is associated with a vortex.

a Galilean transformation to the capillary frame (where the capillary is stationary and the BEC is moving to the right with respect to the capillary), we find that the excitation has energy $\epsilon_p - \vec{p} \cdot \vec{v} = 0$. In this frame the potential produced by the capillary is static and thus cannot transfer energy to the BEC, so

$$v = \frac{\epsilon_p}{p}.$$

But we want the minimum velocity

$$v_c = \min\left(\frac{\epsilon_p}{p}\right). \tag{3.10}$$

This is the critical velocity, or the minimum velocity an obstacle needs to create excitations in the condensate and cause it to lose superfluidity. Anything with a velocity less than v_c will pass through the superfluid without friction. A notable property of superfluids is that the condensate *must* be interacting. This is because without a restoring force, the condensate will simply be destroyed by any object that passes through it. Seen another way: in the non-interacting case, $\epsilon_p = p^2/2m$, so by substituting this into (3.10)

$$v_c = \min\left(\frac{p}{2m}\right) = 0, \tag{3.11}$$

i.e. any velocity will cause a loss of superfluidity.

3.3 Condensates in the Language of Symmetries

3.3.1 $U(1)$ Symmetry

This section closely follows the analysis done in [22] and with reference to [23]. Let $U(n)$ be the n-dimensional unitary group - a group that contains all $n \times n$ complex unitary matrices such that

$$U(n) = \{u \in U_n(\mathbb{C}) : u^\dagger u = 1_{n\times n}\}.$$

Let $\mathbb{T}$ be the circle group

$$\mathbb{T} = \{z \in \mathbb{C} : |z| = 1\},$$

i.e. the group of all complex numbers with absolute value equal to one that form the unit circle in the complex plane. We identify that $\mathbb{T}$ can be parameterized as

$$z = e^{i\phi}.$$

where ϕ is the angle of rotation. We also know that $e^{i\phi}$ is a 1×1 complex matrix such that $e^{i\phi} = u$ because $u^\dagger u = 1_{1\times 1}$. Thus $\mathbb{T} \cong U(1)$ (they are isomorphic) implying $e^{i\phi} \in U(1) : \phi \in \mathbb{R}^1$. If the $U(1)$ group acts on a state $|\psi\rangle$

$$U(1)\,|\psi\rangle = e^{i\phi}\,|\psi\rangle\,, \tag{3.12}$$

this allows us to identify that $U(1)$ characterizes a phase shift $e^{i\phi}$ with phase ϕ of a state $|\psi\rangle$. We then say that $U(1)$ is a (global) symmetry of the system because it leaves $|\psi\rangle$ invariant under a transformation.

This has important implications in physics: Noether's theorem states that for every continuous symmetry of a system, there exists a corresponding conserved charge

$$Q = \int d^3x j^0(x) \tag{3.13}$$

for a conserved four-current j^μ

$$\partial_\mu j^\mu(x) = 0, \tag{3.14}$$

$$j^\mu(x) = \sum_{i=0}^{n} \frac{\partial \mathcal{L}}{\partial(\partial_\mu \psi_i)} \Delta\psi_i. \tag{3.15}$$

Consider a free, non-interacting, complex, scalar field $\psi(\vec{x}, t)$ described by the Lagrangian

$$\mathcal{L}(\psi,\ \psi^*,\ \partial_\mu\psi,\ \partial_\mu\psi^*) = \partial_\mu\psi^*\partial^\mu\psi - m^2|\psi|^2. \tag{3.16}$$

Let us determine what happens when we consider the $U(1)$ symmetry of this field. ψ transforms as

$$\psi \to e^{i\alpha}\psi, \qquad \psi^* \to e^{-i\alpha}\psi^*. \tag{3.17}$$

Under an infinitesimal transformation $\alpha \to \epsilon \ll 1$ and we can do a power expansion of (3.17)

$$\begin{aligned} \psi &\to e^{i\epsilon}\psi \approx (1+\epsilon i)\psi = \psi + \epsilon i\psi \\ \psi^* &\to e^{-i\epsilon}\psi^* \approx (1-\epsilon i)\psi^* = \psi^* - \epsilon i\psi^*. \end{aligned} \tag{3.18}$$

Since $\epsilon i\phi^*$ $(-\epsilon i\psi^*)$ is small, it can be considered as a variation of ψ (ψ^*)

$$\begin{aligned} \delta\psi \equiv \epsilon i\psi \Rightarrow e^{i\epsilon}\psi \approx \psi + \delta\psi \\ \delta\psi^* \equiv \epsilon i\psi^* \Rightarrow e^{-i\epsilon}\psi^* \approx \psi^* - \delta\psi^*. \end{aligned} \tag{3.19}$$

Now (3.15) can be solved using (3.16) and (3.19)

$$\begin{aligned} j^\mu &= \frac{\partial\mathcal{L}}{\partial(\partial_\mu\psi)}\Delta\psi + \frac{\partial\mathcal{L}}{\partial(\partial_\mu\psi^*)}\Delta\psi^* \\ &= i(\psi\partial^\mu\psi^* - \psi^*\partial^\mu\psi). \end{aligned} \tag{3.20}$$

The conserved charge is

$$Q = \int d^3x j^0 = \int d^3x[i(\psi\dot{\psi}^* - \psi^*\dot{\psi})]. \tag{3.21}$$

Now we check that the four-current is conserved

$$\begin{aligned}\partial_\mu j^\mu &= i\partial_\mu(\psi\partial^\mu\psi^* - \psi^*\partial\psi) \\ &= i(\psi\partial_\mu\partial^\mu\psi^* - \psi^*\partial_\mu\partial^\mu\psi).\end{aligned} \tag{3.22}$$

From the Lagrangian, the equations of motion are

$$\begin{aligned}\partial_\mu\frac{\partial\mathcal{L}}{\partial(\partial_\mu\psi)} - \frac{\partial\mathcal{L}}{\partial\psi} &= 0 \\ \Rightarrow \partial_\mu\partial^\mu\psi^* - m^2\psi^* &= 0 \\ \partial_\mu\frac{\partial\mathcal{L}}{\partial(\partial_\mu\psi^*)} - \frac{\partial\mathcal{L}}{\partial\psi^*} &= 0 \\ \Rightarrow \partial_\mu\partial^\mu\psi - m^2\psi &= 0\end{aligned}$$

and we recognize the relationships

$$\begin{aligned}\partial_\mu\partial^\mu\psi^* &= m^2\psi^* \\ \partial_\mu\partial^\mu\psi &= m^2\psi\end{aligned}$$

which we substitute in (4.12)

$$\partial_\mu j^\mu = i(\psi m^2\psi^* - \psi^* m^2\psi) = 0. \tag{3.23}$$

Thus there is a conserved current under a $U(1)$ transformation, meaning that in systems with a $U(1)$ symmetry, there exists a corresponding conserved quantity.

3.3.2 Spontaneous Symmetry Breaking

For certain ground states the symmetries described above are not respected; i.e. when the symmetry is no longer present in the ground state (while it is in the rest of the system) we say that the symmetry is *spontaneously broken*. Let us consider the implications of this.

As a natural extension of the Lagrangian above, we include an interaction term such as $\propto \lambda|\psi|^4$. The original (non-interacting) Lagrangian in the previous section had a global, continuous $U(1)$ symmetry $e^{i\alpha}$ where α is a continuous transformation (identified as the phase). The interaction results in the ground state potential in Figure 3.2. We see that the potential has a continuous set of states that minimize the potential and break the symmetry.

Why do we care?

As discussed before, Noether's theorem states that for every symmetry, there is a conserved quantity (charge). Therefore, when a symmetry is broken, the charge is no longer conserved. Goldstone's theorem states that if a continuous symmetry is spontaneously

broken, then there exists a massless[§] mode - a *Nambu-Goldstone boson*. In the context of BECs and superfluids, the Nambu-Goldstone boson[¶] corresponds to a quasi-particle: the phonon.

There are two important take-aways from this chapter. The first is that Bose-Einstein condensation occurs when the ground state is macroscopically occupied. The second is how symmetries correspond to conserved quantities (or the resulting Nambu-Goldstone bosons when those symmetries are broken). Both of these form the basis for the next chapter where we dive into the concept of superfluid dark matter and its connections to accelerated expansion phenomenology.

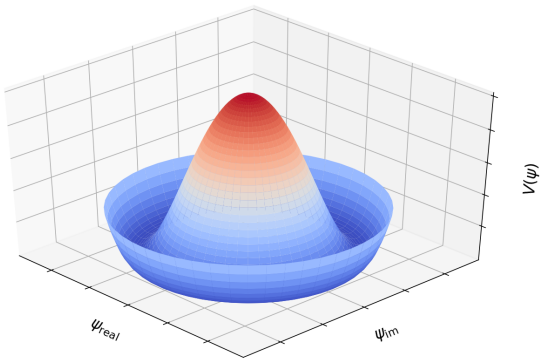

Figure 3.2: The ground state potential that spontaneously breaks the $U(1)$ symmetry of an interacting complex scalar field. Note how there are infinitely many values for the field around the minimum of the potential.

[§]In the literature, *massless* is synonymous with *gapless*.
[¶]Technically in the context of BECs, such bosons are *quasi-Nambu-Goldstone bosons*.

Chapter 4

The Berezhiani-Ferreira-Khoury Model

Because modern cosmology does not have an all-encompassing model for describing dynamics at *all* distance scales - from (sub)galactic scales described by MOND to cosmological distances accurately described by ΛCDM - as well as very little understanding about the elusive nature of dark energy, the field is in need of a unifying model. The Berezhiani-Ferreira-Khoury (BFK) model (as described in [9]) posits that the dark matter in galactic halos is in a Bose-Einstein condensed state. These superfluid halos are able to replicate MOND while uncondensed dark matter outside of the halos agrees with ΛCDM. Additionally, interactions in the halo result in an oscillatory potential that drives late-time cosmic expansion thereby solving the problem of dark energy and cosmic expansion, or in another way: it postulates a unifying framework for the "dark sector" of the Universe and describes dynamics at all distance scales.

Very few of the intermediary calculations presented in this chapter were shown in [9], so it is a goal of this thesis to make them explicit.

4.1 Two-component Dark Matter Superfluid Overview

Let us assume dark matter particles in our model have a mass of $m_{DM} \sim$ eV and that they interact sufficiently strongly to allow them to thermalize in the galactic halo. Given this mass scale, it is reasonable to assume that the dark matter content of the halo is dense and cold enough for it to condense into a Bose-Einstein condensate [24].

In the previous chapter we discussed a Bose-Einstein condensed system where one state is macroscopically occupied. A natural extension of this is to consider a condensed system with two macroscopically occupied states: a ground state and an excited state. By populating this with our dark matter particles, these condensed states are superfluids due to the assumption that they are interacting. The particles in the different energy states will inevitably scatter off one another and in doing so one particle state will be

converted to the other. An analogy to this can be found in atomic physics with *Rabi cycles*[†]. In this process, arbitrarily amounts of atoms in one state transition to another and vice-versa

$$|1\rangle \rightleftharpoons |2\rangle \,.$$

Usually this is accomplished by tuning an oscillatory driving field close to the transition energy of the two states, whereby each oscillation will transport the atoms between the states[25, 26, 27].

Another consequence of these scattering events is the production of phonons. Phonons describe density perturbations (e.g. sound waves) in a superfluid system. Since our model contains two superfluid states, there are two phonon species - one associated with each state, described by the phases θ_1 and θ_2 corresponding the ground and excited states respectively.

In the non-relativistic regime, the phonons are low energy and have long wavelengths. They mediate a long range interaction of the form

$$\mathcal{L}_{int} \propto \frac{\Psi_1^*\Psi_2 + \Psi_2^*\Psi_1}{|\Psi_1||\Psi_2|}, \tag{4.1}$$

where Ψ_i are complex, scalar fields describing the dark matter states. This interaction in turn produces an oscillatory potential

$$V(\theta_2 - \theta_1 + \Delta E t) = M^4 \cos^2\left(\frac{\theta_2 - \theta_1 + \Delta E t}{2}\right); \tag{4.2}$$

this result is derived in the next section. This potential is responsible for late-time cosmic expansion. Thus just by assuming a dark matter-dominated universe where dark matter in galactic halos forms a two-component superfluid, dark energy is the potential produced by the interactions between the phonon species.

4.2 Mathematical Description

4.2.1 The Lagrangian

In this section, we find the Lagrangian describing the two dark matter states with the interaction term (4.1). A good approximation is to describe the dark matter particles as two complex scalar fields. The Lagrangian of two non-interacting, complex, scalar fields is

$$\mathcal{L}_0(\Psi_i,\ \partial\Psi_i) = -\sum_{i=1}^{2}\sqrt{-g}\left(|\partial\Psi_i(\vec{x},\ t)|^2 + m_i^2|\Psi_i(\vec{x},\ t)|^2 + \frac{2m_i^4}{\Lambda_i^4}|\Psi_i(\vec{x},\ t)|^4\right). \tag{4.3}$$

[†]Also known as *Rabi oscillations* or less commonly as a *Rabi coupling*.

$\partial = \partial_\mu = (-\partial_t,\ \partial_j)$ is the four-gradient. Also, $(\partial\Psi)^2 \equiv g^{\mu\nu}\partial_\mu\Psi\partial_\nu\Psi$ and $g = det(g_{\mu\nu})$ and Λ_i are energy cutoffs - they should not be confused with that in ΛCDM. Using polar coordinates

$$\Psi(\vec{x},\ t) = \frac{\rho(\vec{x},\ t)}{\sqrt{2}} e^{i\Theta(\vec{x},\ t)}. \tag{4.4}$$

$\Theta(\vec{x},\ t)$ is the phonon field for the associated dark matter state; it is explicitly time-dependent

$$\Theta(\vec{x},\ t) = mt + \theta(\vec{x},\ t). \tag{4.5}$$

θ is the phonon excitation arising from the background mt. Substitute (4.4) into (4.3), the action is

$$\begin{aligned}
\mathcal{L}_0 &= -\sum_{i=1}^{2} \sqrt{-g} \left\{ \left| \partial \left(\frac{\rho_i}{\sqrt{2}} e^{i\Theta_i} \right) \right|^2 + m_i^2 \left| \frac{\rho_i}{\sqrt{2}} e^{i\Theta_i} \right|^2 + \frac{2m_i^4}{\Lambda_i^4} \left| \frac{\rho_i}{\sqrt{2}} e^{i\Theta_i} \right|^4 \right\} \\
&= -\sum_{i=1}^{2} \frac{\sqrt{-g}}{2} \left\{ \left| e^{i\Theta_i}\partial\rho_i + \rho_i \partial e^{i\Theta_i} \right|^2 + m_i^2 \left| \rho_i e^{i\Theta_i} \right|^2 + \frac{m_i^4}{\Lambda_i^4} \left| \rho_i e^{i\Theta_i} \right|^4 \right\}.
\end{aligned}$$

Since $|\Psi|^2 = (\Psi^*\Psi)$, the first term in the curly braces is

$$\begin{aligned}
&(e^{-i\Theta_i}\partial\rho_i + \rho_i\partial e^{-i\Theta_i})(e^{i\Theta_i}\partial\rho_i + \rho_i\partial e^{i\Theta_i}) \\
&\quad = e^{-i\Theta_i}e^{i\Theta_i}(\partial\rho_i)^2 + \rho_i e^{-i\Theta_i}\partial\rho_i\partial e^{i\Theta_i} + \rho_i e^{i\Theta_i}\partial\rho_i\partial e^{-i\Theta_i} + \rho_i^2\partial e^{i\Theta_i}\partial e^{-i\Theta_i} \\
&\quad = (\partial\rho_i)^2 + \rho_i e^{-i\Theta_i}\partial\rho_i(i)e^{i\Theta_i}(\partial\Theta_i) + \rho_i e^{i\Theta_i}\partial\rho_i(-i)e^{-i\Theta_i}(\partial\Theta_i) \\
&\qquad\qquad + \rho_i^2(-i)e^{-i\Theta_i}(\partial\Theta_i)(i)e^{i\Theta_i}(\partial\Theta_i) \\
&\quad = (\partial\rho_i)^2 + \rho_i^2(\partial\Theta_i)^2;
\end{aligned}$$

the second term is

$$m_i^2\rho_i^2 e^{-i\Theta_i}e^{i\Theta_i} = m_i^2\rho_i^2;$$

and the final term

$$\frac{m_i^4}{\Lambda_i^4}\left[(\rho_i e^{-i\Theta_i})(\rho_i e^{i\Theta_i})\right]^2 = \frac{m_i^4}{\Lambda_i^4}\rho_i^4.$$

Therefore the action is

$$\boxed{\mathcal{L}_0 = -\sum_{i=1}^{2} \sqrt{-g} \left\{ \frac{1}{2}(\partial\rho_i)^2 + \frac{1}{2}\rho_i(\partial\Theta_i)^2 + \frac{1}{2}m_i^2\rho_i^2 + \frac{m_i^4}{2\Lambda_i^4}\rho_i^4 \right\}}. \tag{4.6}$$

In order to find the action for the phonon fields Θ_i, substitute the densities (to leading order in derivatives)

$$\rho_i^2 = \frac{\Lambda_i^4}{2m_i^4}\left(-(\partial\Theta_i)^2 - m_i^2\right) \tag{4.7}$$

into the action (4.6)

$$\mathcal{L}_0 = -\sum_{i=1}^{2}\sqrt{-g}\Bigg\{\frac{1}{2}\left[\partial\left(\frac{\Lambda_i^4}{2m_i^4}\Big(-(\partial\Theta_i)^2 - m_i^2\Big)\right)\right]^2 + \frac{1}{2}\frac{\Lambda_i^4}{2m_i^4}\Big(-(\partial\Theta_i)^2 - m_i^2\Big)(\partial\Theta_i)^2 + \frac{1}{2}m_i^2\frac{\Lambda_i^4}{2m_i^4}\Big(-(\partial\Theta_i)^2 - m_i^2\Big) + \frac{m_i^4}{2\Lambda_i^4}\left[\frac{\Lambda_i^4}{2m_i^4}\Big(-(\partial\Theta_i)^2 - m_i^2\Big)\right]^2\Bigg\}.$$

If we only consider derivatives of first order, then the first term in the curly braces can be excluded. Also, we recognize a common factor of $-\Lambda_i^4/4$

$$\begin{aligned}
\mathcal{L}_0 &= \sum_{i=1}^{2}\sqrt{-g}\frac{\Lambda_i^4}{4}\Bigg\{\frac{1}{m_i^4}\Big((\partial\Theta_i)^2 + m_i^2\Big)(\partial\Theta_i)^2 \\
&\qquad + m_i^2\frac{1}{m_i^4}\Big((\partial\Theta_i)^2 + m_i^2\Big) - \frac{1}{2m_i^4}\Big((\partial\Theta_i)^2 + m_i^2\Big)^2\Bigg\} \\
&= \sum_{i=1}^{2}\sqrt{-g}\frac{\Lambda_i^4}{4}\left\{\frac{\Big((\partial\Theta_i)^2 + m_i^2\Big)\Big[2(\partial\Theta_i)^2 + 2m_i^2 - \Big((\partial\Theta_i)^2 + m_i^2\Big)\Big]}{2m_i^2}\right\} \\
&= \sum_{i=1}^{2}\sqrt{-g}\frac{\Lambda_i^4}{8}\left\{\frac{(\partial\Theta_i)^4}{m_i^4} + \frac{2m_i^2(\partial\Theta_i)^2}{m_i^4} + 1\right\} \\
&= \sum_{i=1}^{2}\sqrt{-g}\frac{\Lambda_i^4}{8}\left\{\frac{(\partial\Theta_i)^2}{m_i^2} + 1\right\}^2.
\end{aligned} \tag{4.8}$$

We now choose to work in the non-relativistic limit. This implies that the phonon excitations go as

$$\dot{\theta}_i \ll m_i \tag{4.9}$$

and the metric goes to the weak-field Newtonian limit

$$g_{\mu\nu} = \begin{pmatrix} -(1+2\Phi) & 0 & 0 & 0 \\ 0 & (1-2\Phi) & 0 & 0 \\ 0 & 0 & (1-2\Phi) & 0 \\ 0 & 0 & 0 & (1-2\Phi) \end{pmatrix} \tag{4.10}$$

where $\Phi = \Phi(\vec{x}, t)$ is the gravitational potential. In this limit, (4.8) simplifies

$$\begin{aligned}
\mathcal{L}_0 &= \sum_{i=1}^{2} \sqrt{-g}\frac{\Lambda_i^4}{8}\left\{\frac{1}{m_i^2}\left(g^{\mu\nu}\partial_\mu\Theta_i\partial_\nu\Theta_i\right)+1\right\}^2 \\
&= \sum_{i=1}^{2} \frac{\Lambda_i^4}{8}\left\{\frac{1}{m_i^2}\left(g^{00}\partial_0\Theta_i\partial_0\Theta_i + g^{kl}\partial_k\Theta_i\partial_l\Theta_i\right)+1\right\}^2 \\
&= \sum_{i=1}^{2} \frac{\Lambda_i^4}{8}\Big\{\frac{1}{m_i^2}\Big[(-1+2\Phi)\partial_t(m_it+\theta_i)\partial_t(m_it+\theta_i) \\
&\qquad\qquad + (1+2\Phi)\partial_k(m_it+\theta_i)\partial_l(m_it+\theta_i)\Big]+1\Big\}^2 \\
&= \sum_{i=1}^{2} \sqrt{-g}\frac{\Lambda_i^4}{8}\left\{\frac{1}{m_i^2}\left[(-1+2\Phi)(m_i^2+2\dot{\theta}_i m_i+\dot{\theta}_i^2)+(1+2\Phi)(\vec{\nabla}\theta_i)^2\right]+1\right\}^2 \\
&= \sum_{i=1}^{2} \frac{\Lambda_i^4}{8}\Big\{\frac{1}{m_i^2}\Big[-m_i^2-2\dot{\theta}_i m_i-\dot{\theta}_i^2+2\Phi m_i^2+4\Phi\dot{\theta}_i m_i+2\Phi\dot{\theta}_i^2 \\
&\qquad\qquad + (\vec{\nabla}\theta_i)^2+2\Phi(\vec{\nabla}\theta_i)^2\Big]+1\Big\}^2 \\
&= \sum_{i=1}^{2} \frac{\Lambda_i^4}{8}\left\{-1-\frac{2\dot{\theta}_i}{m_i}-\frac{\dot{\theta}_i^2}{m_i^2}+2\Phi+\frac{4\Phi\dot{\theta}_i}{m_i}+\frac{2\Phi\dot{\theta}_i^2}{m_i^2}+\frac{(\vec{\nabla}\theta_i)^2}{m_i^2}+\frac{2\Phi(\vec{\nabla}\theta_i)^2}{m_i^2}+1\right\}^2 \\
&= \sum_{i=1}^{2} \frac{\Lambda_i^4}{8}\frac{4}{m_i^2}\left\{-\left[\dot{\theta}_i+\frac{\dot{\theta}_i^2}{2m_i}-\Phi m_i-2\Phi\dot{\theta}_i-\frac{\Phi\dot{\theta}_i^2}{m_i}-\frac{(\vec{\nabla}\theta_i)^2}{2m_i}-\frac{\Phi(\vec{\nabla}\theta_i)^2}{m_i}\right]\right\}^2.
\end{aligned}$$

Because of the non-relativistic limit and because Φ is small, the non-interacting Lagrangian term approximates to

$$\boxed{\mathcal{L}_0 = \sum_{i=1}^{2}\frac{\Lambda_i^4}{2m_i^2}\left\{\dot{\theta}_i - \Phi m_i - \frac{(\vec{\nabla}\theta_i)^2}{2m_i}\right\}^2}. \tag{4.11}$$

4.2.2 The Conserved Currents

The conserved currents are

$$j_i^\mu = \frac{\partial\mathcal{L}}{\partial(\partial_\mu\Psi_i)}\Delta\Psi_i + \frac{\partial\mathcal{L}}{\partial(\partial_\mu\Psi_i^*)}\Delta\Psi_i^*.$$

The Lagrangian of a complex scalar field goes as $\mathcal{L}\sim|\partial\Psi|^2$, so

$$\begin{aligned}
j_i^\mu &= \frac{\partial}{\partial(\partial_\mu\Psi_i)}\Big\{\big(\partial_\nu\Psi_i^*\big)\big(\partial^\nu\Psi_i\big)\Big\}\Delta\Psi_i + \frac{\partial}{\partial(\partial_\mu\Psi_i^*)}\Big\{\big(\partial_\nu\Psi_i^*\big)\big(\partial^\nu\Psi_i\big)\Big\}\Delta\Psi_i^* \\
&= \partial^\mu\Psi_i^*\Delta\Psi + \partial^\mu\Psi_i\Delta\Psi_i^*.
\end{aligned}$$

We can perform an infinitesimal transformation on the wave function such that $\Psi \to \Psi + \alpha\Delta\Psi$ and $\alpha\Delta\Psi = i\alpha\Psi$, implying

$$\Delta\Psi = i\Psi$$

and

$$\Delta\Psi^* = -i\Psi^*.$$

Therefore

$$\begin{aligned} j_i^\mu &= \partial^\mu\Psi_i^* i\Psi_i + \partial^\mu\Psi_i\,(-i)\,\Psi_i^* \\ &= i(\Psi_i\partial^\mu\Psi_i^* - \Psi_i^*\partial_\mu\Psi_i) \\ &= -i(\Psi_i^*\partial^\mu\Psi_i - \Psi_i\partial^\mu\Psi_i^*). \end{aligned} \tag{4.12}$$

Substituting the wave function in polar coordinates (4.4) and its complex conjugate into (4.12)

$$\begin{aligned} j_i^\mu &= -i\left\{\frac{\rho_i}{\sqrt{2}}e^{-i\Theta_i}\partial^\mu\left[\frac{\rho_i}{\sqrt{2}}e^{i\Theta_i}\right] - \frac{\rho_i}{\sqrt{2}}e^{i\Theta_i}\partial^\mu\left[\frac{\rho_i}{\sqrt{2}}e^{-i\Theta_i}\right]\right\} \\ &= -i\Bigg\{\frac{\rho_i}{2}e^{-i\Theta_i}\left[e^{i\Theta_i}\partial^\mu\rho_i + \rho_i\partial^\mu e^{i\Theta_i}\right] \\ &\qquad - \frac{\rho_i}{2}e^{i\Theta_i}\left[e^{-i\Theta_i}\partial^\mu\rho_i + \rho_i\partial^\mu e^{-i\Theta_i}\right]\Bigg\} \\ &= -i\Bigg\{\frac{\rho_i}{2}\left[e^{i\Theta_i}e^{-i\Theta_i}\partial^\mu\rho_i + e^{-i\Theta_i}\rho_i ie^{i\Theta_i}\partial^\mu\Theta_i\right] \\ &\qquad - \frac{\rho_i}{2}\left[e^{i\Theta_i}e^{-i\Theta_i}\partial^\mu\rho_i + \rho_i e^{i\Theta_i}(-i)e^{-i\Theta_i}\partial^\mu\Theta_i\right]\Bigg\} \\ &= -i\left\{\frac{\rho_i}{2}\partial^\mu\rho_i + i\frac{\rho_i^2}{2}\partial^\mu\Theta_i - \frac{\rho_i}{2}\partial^\mu\rho_i + i\frac{\rho_i^2}{2}\partial^\mu\Theta_i\right\} \\ &= -i\left\{i\rho_i^2\partial^\mu\Theta_i\right\} \\ &= \boxed{\rho_i^2\partial^\mu\Theta_i}. \end{aligned} \tag{4.13}$$

4.2.3 Including an Interaction Term

The theory would be incomplete without an interaction term; we introduce one as

$$\mathcal{L}_{int} \propto -\frac{\Psi_1^*\Psi_2 + \Psi_2^*\Psi_1}{|\Psi_1||\Psi_2|}. \tag{4.14}$$

This term spontaneously breaks the global $U(1)\times U(1)$ symmetry to a global $U(1)$ symmetry. In the next subsection, we will comment on the implications of this. Substitute

the polar wave function (4.4) into this interaction term

$$\begin{aligned}\propto &- \left(\frac{\rho_1}{\sqrt{2}}e^{-i\Theta_1}\frac{\rho_2}{\sqrt{2}}e^{i\Theta_2} + \frac{\rho_2}{\sqrt{2}}e^{-i\Theta_2}\frac{\rho_1}{\sqrt{2}}e^{i\Theta_1}\right)\left(\left|\frac{\rho_1}{\sqrt{2}}e^{i\Theta_1}\right|\left|\frac{\rho_2}{\sqrt{2}}e^{i\Theta_2}\right|\right)^{-1} \\ &= -\left(\frac{e^{i(\Theta_2-\Theta_1)} + e^{-i(-\Theta_1+\Theta_2)}}{2}\right)\left(\left|\frac{e^{i(\Theta_1+\Theta_2)}}{2}\right|\right)^{-1} \\ &= \frac{-\cos(\Theta_2-\Theta_1)}{|\cos(\Theta_1+\Theta_2)+i\sin(\Theta_1+\Theta_2)|}.\end{aligned}$$

The magnitude of the denominator is

$$\sqrt{\big[\cos(\Theta_1+\Theta_2)+i\sin(\Theta_1+\Theta_2)\big]\big[\cos(\Theta_1+\Theta_2)-i\sin(\Theta_1+\Theta_2)\big]} = 1.$$

Therefore the interaction is proportional to

$$\mathcal{L}_{int} \propto -\cos(\Theta_2-\Theta_1)$$

such that there is some constant D

$$\mathcal{L}_{int} = -D\cos(\Theta_2-\Theta_1).$$

The authors of [9] add a constant (c) to the interaction such that the vacuum energy vanishes at the potential's minimum:

$$\mathcal{L}_{int} = -D\cos(\Theta_2-\Theta_1) + c.$$

By equating D to $M^4/2$ and $c = -M^4/2$ the interaction is

$$\begin{aligned}\mathcal{L}_{int} &= -\frac{M^4}{2}\cos(\Theta_2-\Theta_1) - \frac{M^4}{2} \\ &= -M^4\left(\frac{\cos(\Theta_2-\Theta_1)+1}{2}\right) \\ &= \boxed{-M^4\cos^2\left(\frac{\Theta_2-\Theta_1}{2}\right) = -V(\Theta_2-\Theta_1)},\end{aligned} \tag{4.15}$$

where the last line comes from the cosine half-angle formula. This is simplified using the equation for the phonon field (4.5)

$$\begin{aligned}\Theta_2-\Theta_1 &= m_2t + \theta_2 - m_1t - \theta_1 \\ &= \theta_2 - \theta_1 + \Delta E t\end{aligned} \tag{4.16}$$

where $\Delta E \equiv m_2 - m_1$ is the energy difference between the two states. Therefore the full Lagrangian is

$$\boxed{\mathcal{L} = \sum_{i=1}^{2}\frac{\Lambda_i^4}{2m_i^2}\left\{\dot{\theta}_i - \Phi m_i - \frac{(\vec{\nabla}\theta_i)^2}{2m_i}\right\}^2 - V(\theta_2-\theta_1+\Delta E t)}. \tag{4.17}$$

4.2.4 Background Evolution

In order to better understand the nature of cosmic expansion in this model, we can derive the Friedmann equation for this model. The total energy density of the superfluid can be expressed as

$$\begin{aligned}\rho &= m_1\frac{\partial P_1}{\partial X_1} + m_2\frac{\partial P_2}{\partial X_2} + V(\Delta E t)\\ &= \frac{1}{2}(m_1+m_2)\left(\frac{\partial P_1}{\partial X_1}+\frac{\partial P_2}{\partial X_2}\right) + \frac{1}{2}\Delta E\left(-\frac{\partial P_1}{\partial X_1}+\frac{\partial P_2}{\partial X_2}\right) + V(\Delta E t).\end{aligned} \tag{4.18}$$

Note that the ΔE term in Equation 4.4 of [9] is written as

$$\sim \frac{1}{2}\Delta E(P_{1\ ,X_1} - P_{2\ ,X_2}),$$

which is incorrect; the corrected term is expressed in (4.18). The pressure is the Lagrangian density

$$\mathcal{P} = \mathcal{L} = P_1(X_1) + P_2(X_2) - V(\Delta E t). \tag{4.19}$$

The first Friedmann equation [11] is

$$H^2 = \left(\frac{\dot{a}}{a}\right)^2 = \frac{8\pi G}{3}\rho. \tag{4.20}$$

By definition, the reduced Planck mass $M_{pl}^2 = 1/8\pi G$ so that (4.20) becomes

$$H^2 = \frac{\rho}{3M_{pl}^2}$$

and by substituting (4.18), our final equation is

$$\boxed{3M_{pl}^2H^2 = \frac{1}{2}(m_1+m_2)\left(\frac{\partial P_1}{\partial X_1}+\frac{\partial P_2}{\partial X_2}\right) + \frac{1}{2}\Delta E\left(-\frac{\partial P_1}{\partial X_1}+\frac{\partial P_2}{\partial X_2}\right) + V(\Delta E t)}. \tag{4.21}$$

Note again that the mistake mentioned above is propagated into Equations (5.1) - (5.2) in their definition of ρ_-

$$\rho_- \equiv \frac{1}{2}\Delta E(P_{1\ ,X_1} - P_{2\ ,X_2})$$

and is corrected in the above boxed equation (these do not effect their final expressions or results). The second Friedmann equation is the time derivative of the first

$$2H\dot{H} = \frac{\dot{\rho}}{3M_{pl}^2}.$$

We can use the standard expression for the conservation of energy to get an expression for $\dot{\rho}$

$$\begin{aligned}\dot{\rho} &= 3H(p+\rho) = 0 \\ \Rightarrow 2\dot{H} &= -\frac{p+\rho}{M_{pl}^2}.\end{aligned}$$

As before, we substitute in the total energy density ρ, and the pressure $\mathcal{P} = p$

$$\begin{aligned}2\dot{H}M_{pl}^2 = -\Bigg[&P_1(X_1) + P_2(X_2) - V(\Delta Et) + \frac{1}{2}(m_1+m_2)\left(\frac{\partial P_1}{\partial X_1} + \frac{\partial P_2}{\partial X_2}\right) \\ &+ \frac{1}{2}\Delta E\left(-\frac{\partial P_1}{\partial X_1} + \frac{\partial P_2}{\partial X_2}\right) + V(\Delta Et)\Bigg].\end{aligned}$$

We recognize that in the non-relativistic limit $m\partial P/\partial X \gg P$

$$\boxed{2\dot{H}M_{pl}^2 = -\left[\frac{1}{2}(m_1+m_2)\left(\frac{\partial P_1}{\partial X_1} + \frac{\partial P_2}{\partial X_2}\right) + \frac{1}{2}\Delta E\left(-\frac{\partial P_1}{\partial X_1} + \frac{\partial P_2}{\partial X_2}\right)\right]}. \tag{4.22}$$

Finally, by summing the first (4.21) and second equations (4.22), we get an equation for the evolution of the background cosmology

$$\boxed{2\dot{H} + 3H^2 = \frac{V(\Delta Et)}{M_{pl}^2}}. \tag{4.23}$$

We now have the necessary background to test the BFK model. The analysis begins with (4.23) as this maps the expansion of the universe with the interaction potential V.

Chapter 5

Tests of the BFK Model

We now perform three test of the BFK model. First, we plot the evolution of the Hubble parameter in both BFK and ΛCDM - both models agree until late times when BFK begins to oscillate. Next, we calculate the luminosity distance and compare the results to supernova observations from SDSS-II and SNLS and find statistically significant energy gaps $\Delta\epsilon$. Finally, we calculate the CMB shift parameter, which also allows us to constrain Ω_m in BFK.

5.1 Evolution of the Hubble Parameter

We start with the Friedmann equation (4.23) as found in the last section

$$2\dot{H} + 3H = \frac{V(\Delta Et)}{M_{pl}^2} \tag{5.1}$$

with the potential

$$V(\Delta Et) = M^4 \cos^2\left(\frac{\Delta Et}{2}\right) \tag{5.2}$$

where $M_{pl}^2 = \sqrt{1/8\pi G}$ is the reduced Planck mass, ΔE is the energy gap between the two distinguishable superfluid dark matter states, and $M^4 = 3H_0^2 M_{pl}^2$ is a scale factor that sets the amplitude of the potential. Substituting (5.2) into (5.1)

$$\begin{aligned} 2\dot{H} + 3H^2 &= \frac{M^4 \cos^2\left(\frac{\Delta Et}{2}\right)}{M_{pl}^2} \\ 2\frac{dH}{dt} + 3H^2 &= 3H_0^2 M_{pl}^2 \cos^2\left(\frac{\Delta Et}{2}\right)\frac{1}{M_{pl}^2} \\ &= 3H_0^2 \cos^2\left(\frac{\Delta Et}{2}\right). \end{aligned}$$

Now let τ be a dimensionless time parameter such that

$$\tau \equiv H_0 t \tag{5.3}$$

$$\Rightarrow 2H_0 \frac{dH}{d\tau} + 3H^2 = 3H_0^2 \cos^2\left(\frac{\Delta E \tau}{2H_0}\right).$$

Multiply by $1/H_0^2$

$$\frac{2}{H_0}\frac{dH}{d\tau} + 3\left(\frac{H}{H_0}\right)^2 = 3\cos^2\left(\frac{\Delta E \tau}{2H_0}\right). \tag{5.4}$$

Let h be a dimensionless Hubble parameter

$$h \equiv \frac{H}{H_0} \tag{5.5}$$

$$\Rightarrow \boxed{2\frac{dh}{d\tau} + 3h^2 = 3\cos^2\left(\frac{\tau}{10}\right)} \tag{5.6}$$

where $\Delta E/2H_0 = .1$ at late times (from FIG. 1 of [9]). A plot of (5.6) for $\tau = .01$ to 10 is represented in Figure 5.1. It is in excellent agreement with ΛCDM from early times to the present (where $h \approx 1$ and $\tau = 1$), assuming that the dark energy component of ΛCDM dominates at late times ($\Omega_\Lambda = .99$, $\Omega_m = .01$, $\Omega_b = 0$, and $\Omega_r = 0$). This test was also performed by Ferreira et al. and our results also agree with theirs.

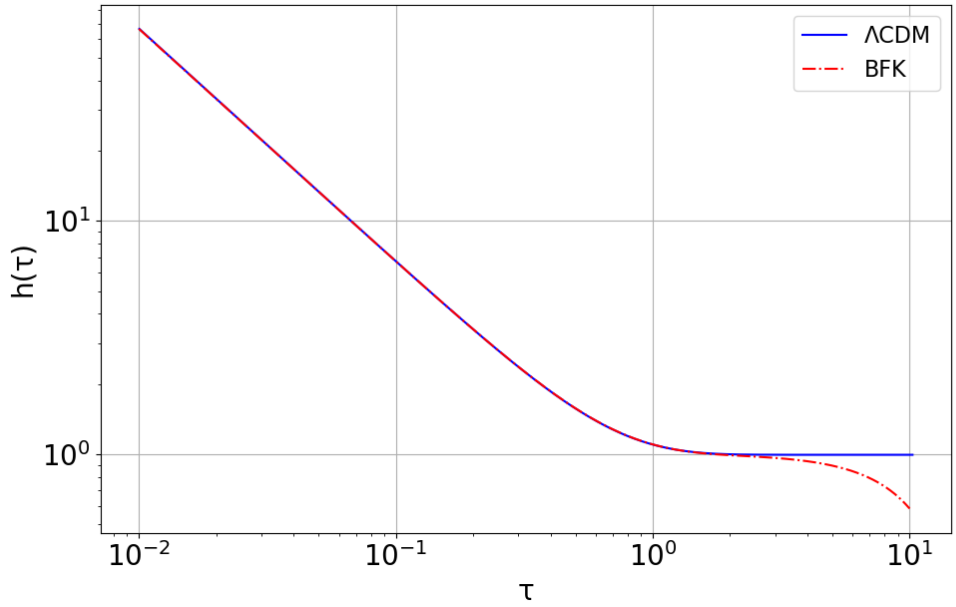

Figure 5.1: A comparison between the ΛCDM and BFK models. They are in agreement until today if ΛCDM is dominated by dark energy at late times. This is a reproduction of Figure 1 in [9].

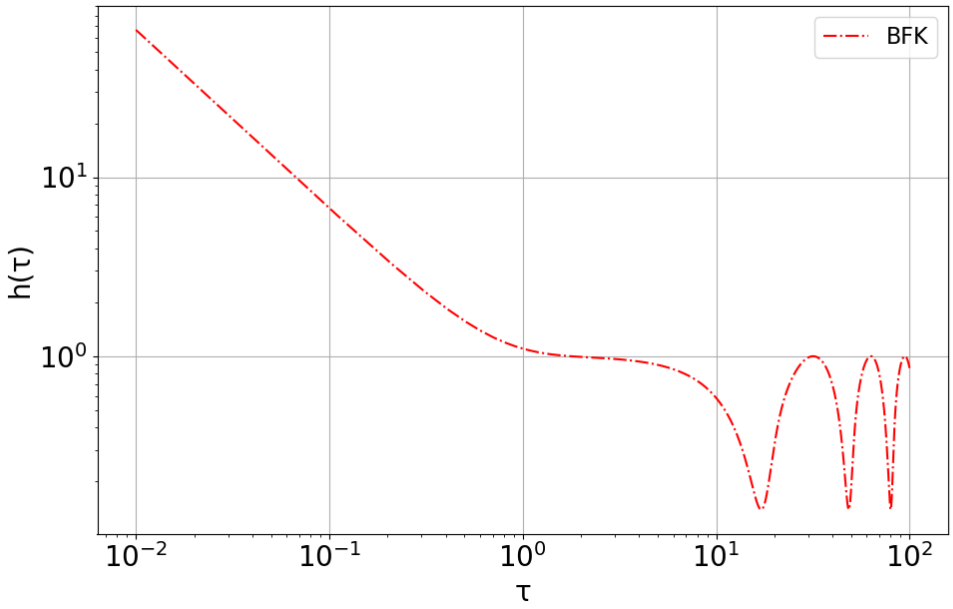

Figure 5.2: A plot of the Hubble parameter in BFK to very late time. It exhibits an oscillatory behavior due to the cosine in the potential.

By evolving h_{BFK} further in time, it begins to oscillate because of the cosine potential - see Figure 5.2. From this plot, we can make two inferences. First, h_{BFK} will almost always be lower than $h_{\Lambda\text{CDM}}$, implying that a ΛCDM universe will become greater in extent than a BFK universe. Second, a BFK universe will go through ever-shortening periods of accelerating and decelerating expansion, but it will never contract. Thus, similar to universe populated with a vacuum energy, a BFK universe will expand forever after dark energy dominates the energy density.

5.2 Luminosity Distance

We will now test the model with observations, something that was not done in [9]. In order to consider distance measurements at large redshifts, it is convenient to define the *luminosity distance*, d_L. This is a relationship between the *absolute luminosity*, L - the total energy emitted from a source per second - the *proper distance*, d - the distance measured by an observer in locally Cartesian coordinates - and the *apparent luminosity*, l - the luminosity of an object measured at a distance d. One can write this relation as

$$l = \frac{L}{4\pi d_L^2}; \quad d_L \equiv a(t_0)(1+z)r. \tag{5.7}$$

From the definition of d_L, one can see that it is dependent on the redshift of the source, which should be expected if we are considering distant objects. The luminosity distance reduces to r at very low redshifts, as one would expect, because the expansion of space at low z has a negligible effect on the luminosity.

Following a brief analysis as given in [11], one finds the equation for the luminosity distance in a ΛCDM universe

$$\boxed{d_L(z) = \frac{1+z}{H_0} \int_{1/(1+z)}^{1} \frac{dx}{x^2\sqrt{\Omega_m x^{-3} + \Omega_\Lambda}}} \tag{5.8}$$

or generally as

$$d_L = \frac{1+z}{H_0} \int_0^z \frac{dz'}{H(z')/H_0}. \tag{5.9}$$

In order to test the BFK model, we used type Ia supernova (SN Ia) data compiled in [28] from the Sloan Digital Sky Survey-II (SDSS-II) and the Supernova Legacy Survey (SNLS). Together they provide measurements on 740 supernovae from $z = .01$ to $z = 1.3$ and allow us to compare luminosity distances in different models. Type 1a supernovae are regarded as "standard candles" in that they produce known and generally uniform light curves; they are thus predictable and make excellent calibration tools. The authors provide the supernova data as distance moduli, which can be well approximated in 31 bins (μ_b). The distance modulus for any cosmological model can be found with

$$\mu = 5\log_{10}(d_L/10\text{pc}). \tag{5.10}$$

In calculating d_L for ΛCDM, we assume $\Omega_m = .3$, $\Omega_\Lambda = .7$, and $H_0 = 70$ and we integrate (5.8) before multiplied by a factor of 1×10^6 Mpc $\cdot$ c to convert to physical units. Getting the luminosity distance for the BFK model is somewhat more involved. After solving (5.6) for $h(\tau)$, we multiply by H_0 to get a Hubble parameter in terms of cosmic time t_c. Then we use the relation

$$H = \frac{\dot{a}(t_c)}{a(t_c)} = \frac{1}{a}\frac{da}{dt_c} \tag{5.11}$$

and integrate over t_c to get $a(t_c)$. Finally, the luminosity distance is

$$d_L(z) = \frac{1+z}{H_0} \int_{t_c}^{t_0} \frac{dt}{a(t)}. \tag{5.12}$$

We find that the luminosity distance in BFK is identical to that of ΛCDM as in Figure 5.3.

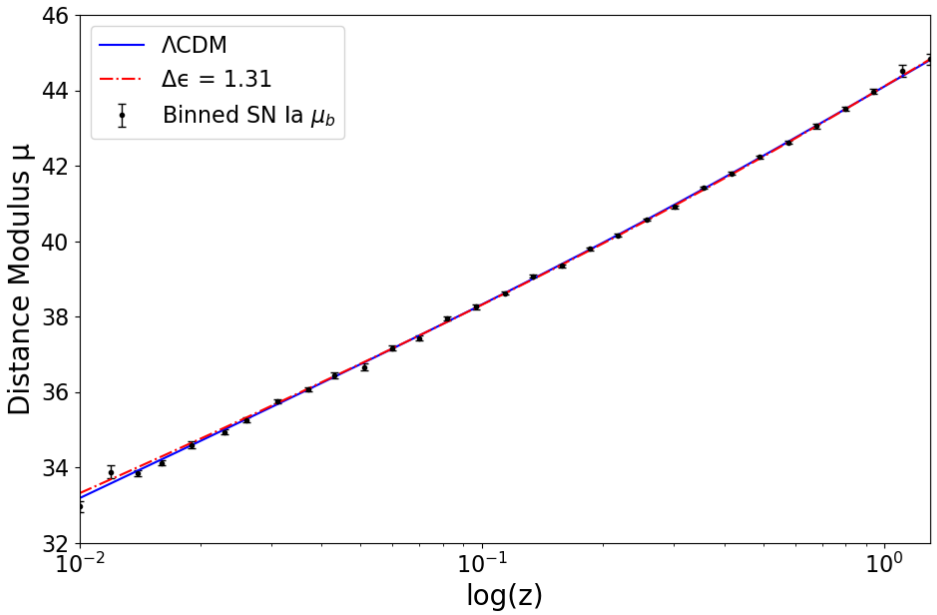

Figure 5.3: The binned SN Ia distance modulus plotted with the ΛCDM and best-fit BFK distance moduli.

Parameter estimation and goodness-of-fit

Since the assumption made about ΔE in (5.6) is only for late times, we reintroduce it to do analysis in the present; we start with the potential in (5.4)

$$3\cos\left(\frac{\Delta E\tau}{2H_0}\right)^2$$

and as before define a dimensionless energy

$$\Delta\epsilon = \frac{\Delta E}{H_0} \tag{5.13}$$

$$\Rightarrow 2\frac{dh}{d\tau} + 3h^2 = 3\cos\left(\frac{\Delta\epsilon\tau}{2}\right)^2. \tag{5.14}$$

$\Delta\epsilon$ is now a free parameter in the model, which we will minimize in order to best fit the SN Ia data. In [28], they provide a χ^2 calculation for the goodness-of-fit of a cosmological model's luminosity distance $D_L(z,\ \theta)$ for some set of parameters θ; in our case $\theta = \Delta\epsilon$:

$$\chi^2(\Delta\epsilon,\ M) = r^\dagger C_b^{-1} r, \tag{5.15}$$

$$r = \mu_b - M - 5\log D_L(z_b,\ \Delta\epsilon). \tag{5.16}$$

M is a free normalization parameter that minimizes χ^2 for each $\Delta\epsilon$. C_b is a covariance matrix provided by [28] in Appendix F. Before going further, χ^2 tests will be briefly defined. In a χ^2 test, one must specify a null hypothesis $\bar{H}_0$ (we will use over-bars to avoid confusion with the Hubble constant) and an alternative hypothesis $\bar{H}_1$. $\bar{H}_0$ holds when the difference between the expected and observed values is zero ($\chi^2 = 0$). We say that $\bar{H}_0$ is rejected in favor of $\bar{H}_1$ when the expected and observed values are significantly different. In our case

$$\bar{H}_0 : \text{For a given } \Delta\epsilon, \text{ the BFK model describes SDSS-II SN Ia observations}$$

and

$$\bar{H}_1 : \text{The BFK model does not describe SN Ia observations.}$$

In determening the statistical significance of a χ^2 test, one must also specify two more values: the degrees of freedom (d.o.f.) and α (a.k.a. the *p-value*). d.o.f. is simply one less than the number of categories or bins in an experiment; there are 31 distance moduli bins in the SDSS data set, so we are working with $31 - 1 = 30$ d.o.f. The standard value for determining statistical significance is $\alpha = .05$ - there is a 5% chance that, given a random observation, the null hypothesis is rejected erroneously.

It is then simply a matter of looking up the cut-off χ^2 value in a χ^2 Table. For example, we find that $\chi^2 = 33.05$ for the mass gap $\Delta\epsilon = 1.286$ with $M = .02903$. In [29], the threshold for d.o.f. $= 30$ and $\alpha = .05$ is $\chi^2 = 43.773$: values higher than this reject the null hypothesis and are statistically insignificant, while those lower are statistically significant. A table showing M and χ^2 for ΛCDM and the thirty $\Delta\epsilon$ values we used is shown in Appendix A. In our analysis, we find statistically significant $\Delta\epsilon$ values in the range $.49 \lesssim \Delta\epsilon \lesssim 1.79$. These were determined from an initial range of 0 to 25. the reasoning for which is explained in the next section. For comparison $\chi^2_{\Lambda CDM} = 33.65$ with $M = 0$, which is also statistically significant.

5.3 The CMB Shift Parameter

The shift parameter, $\mathcal{R}$, is related to the position of the first peak in the CMB power spectrum. It is used in tests of dark energy models where calculating the full CMB power spectrum would be difficult or impossible - it is likewise easier to calculate one value from a single integral. It is defined as

$$\mathcal{R} = \sqrt{\Omega_m} H_0 \int_0^{z_r} \frac{dz}{H(z)} \tag{5.17}$$

and for ΛCDM is

$$\mathcal{R}_{\Lambda CDM} = \sqrt{\Omega_m} H_0 \int_0^{z_r} \frac{dz}{\sqrt{\Omega_m (1+z)^3 + \Omega_\Lambda}} \tag{5.18}$$

assuming that the recombination redshift $z_r \sim 1000$. We take the accepted value to be (at 1σ) $\mathcal{R} = 1.71 \pm .03$ from the three-year Wilkinson Microwave Anisotropy Probe

(WMAP) survey (which we reference from [30]). Using H calculated for ΛCDM in the luminosity distance integral, $\mathcal{R}_{\Lambda CDM} = 1.74(7)$ with the fiducial values $\Omega_m = .3$ and $H_0 = 100h_0 = 70$, which accounts for why $\mathcal{R}_{\Lambda CDM}$ is somewhat high because we make no attempt to find the best-fit values of Ω_m and H_0.

Calculating $\mathcal{R}$ in BFK

$\mathcal{R}_{BFK}$ is found by integrating over H found from (5.11) in (5.17). In this calculation we identify three free parameters: $\Delta\epsilon$, Ω_m, and h_0. Ferreira et al. (2019) assume the field is slowly rolling, which gives us a constraint on $\Delta\epsilon$

$$\Delta E \sim H_0 \tag{5.19}$$

implying

$$.01 \lesssim \Delta\epsilon \lesssim 2. \tag{5.20}$$

Using this range, we create grids of $\mathcal{R}$ values where each square is characterized by a different set of $(\Delta\epsilon,\ \Omega_m,\ h_0)$. By only considering the accepted values of $\mathcal{R}$ from WMAP, then the parameter space in the BFK model is shown in Figure 5.4 - i.e. the accepted values of $\mathcal{R}$ are represented by the red-blue contour for various Ω_m and $\Delta\epsilon$.

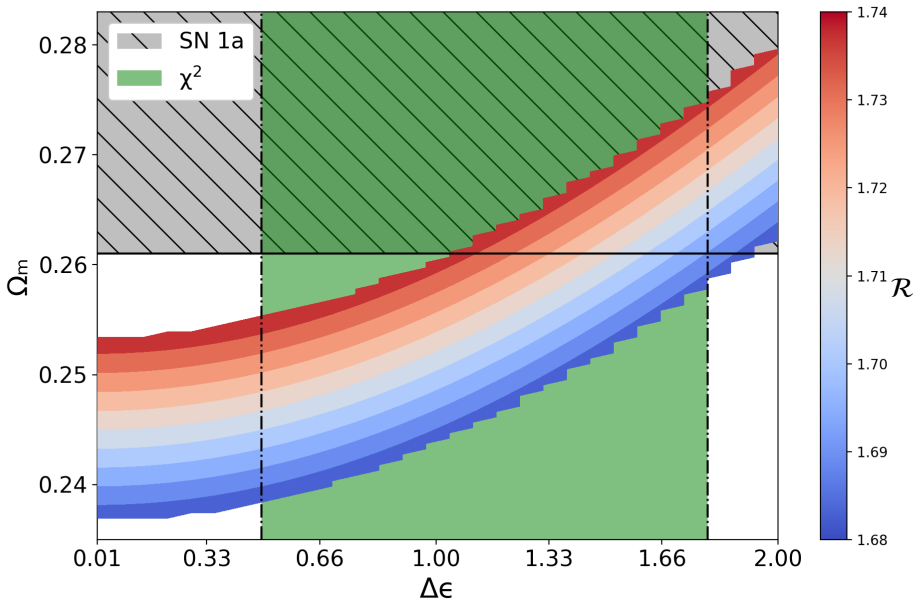

Figure 5.4: $(\Delta\epsilon,\ \Omega_m,\ h_0)$ parameter space in the BFK model with $\Delta\epsilon$ bounds from the χ^2 test (green region bounded by the vertical, dash-dot lines) and Ω_m bounds from SN 1a observations (gray, hatched region bounded from below by the solid, horizontal line).

A couple inferences can be made from this: first, both the Ω_m and $\Delta\epsilon$ parameters are extremely degenerative and require further constraints. Second, we find that h_0 has a negligible effect on $\mathcal{R}$, so we simply set it to .70 for the rest of the analysis.

Using the χ^2 test from the previous section, the statistically significant values of $\Delta\epsilon$ are $.49 \lesssim \Delta\epsilon \lesssim 1.79$. This range of values also substantiates the slow-roll claim (5.19) from [9]. We represent the allowed values from this restraint by the green region in Figure 5.4 bounded by the dash-dot lines. We also include bounds from the SDSS/SNLS study as the gray, hatched region, bounded from below by the solid, black line. From the constrained $\Delta\epsilon$ and $\mathcal{R}$ values, find that $\Omega_m = .255 \pm .00950$ in a BFK universe, which is in agreement with $\Omega_m = .295 \pm .034$ from SDSS.

Chapter 6

Conclusion

In this thesis we investigated the description of dark matter as two light, interacting, Bose-Einstein condensed, axion-like, complex, scalar fields, which at late-times produces a potential through contact interactions that seems to acts like a vacuum energy and mimics the accelerated expansion of the universe as observed today. Specifically, we began this analysis by deriving the foundational equations in Ferreira et al.'s original article, including: the full Lagrangian with the two fields described by their phases, the conserved currents before the introduction of the interaction potential and the spontaneous symmetry breaking $U(1) \times U(1) \to U(1)$, and the background evolution as described by the Hubble parameter. The details of these calculations are missing in the BFK paper.

6.1 Summary of Results

We performed three model tests: the evolution of the Hubble parameter was plotted to very late times and compared to ΛCDM (Section 5.1); the luminosity distance was calculated out to a redshift of $z = 1.3$ for various energy gap values ($\Delta\epsilon$) and then compared to ΛCDM predictions and binned SN Ia distance moduli from SDSS-II (Section 5.2); the CMB shift parameter was also found for a large parameter space constituted of ($\Delta\epsilon$, Ω_m, h_0), and together with the luminosity distance puts constraints on $\Delta\epsilon$ and Ω_m (Section 5.3).

We summarize our results here for convenience: from the luminosity distance goodness-of-fit χ^2 test, the statistically significant energy gaps are $\Delta\epsilon = 1.14 \pm .65$. Then from the CMB shift parameter (assuming $\mathcal{R} = 1.71 \pm .03$), we can constrain the parameter space to find $\Omega_m = .255 \pm .0095$. Remarkably, this agrees with the value of Ω_m found from SDSS-II SN survey: $\Omega_m = .295 \pm .035$ [28].

The double-edged sword of the accuracy and agreement of BFK's parameter space in regards to observation makes it, at least in our tests, indistinguishable from ΛCDM. There is no "smoking gun" in this context that distinguishes it from ΛCDM's already

broad successes. Between d_L, $\chi^2_{d_L}$, and Ω_m, BFK and ΛCDM are essentially identical. One must investigate specific situations where ΛCDM breaks-down to glean any useful information. This is in no way a strike against BFK: on the contrary, passing these basic (but absolutely essential) tests gives us confidence to move forward and apply more rigorous analysis, while assuring us that we might not be wasting our time as we wade through the veritable swampland of contentious dark energy models. This brings us then to the next steps in testing and constraining this model.

6.2 Improvements and Future Work

In further analyzing the BFK model, there are two avenues down which one can proceed: where ΛCDM is deficient as mentioned in Chapter 1, or situations where the physics is extremely well-studied with stringent observational constraints. An example of the latter is the CMB: Ferreira et al. provide equations for linear density perturbations, so in principle it should be possible to calculate the CMB power spectrum. In practice this may or may not be possible, but the constraint it places on the model are invaluable.

The preliminary BFK model was formulated at zero-temperature - this is an idealized assumption. By including finite-temperature effects, the ground state energy of the model would undoubtedly be changed, leading to, among other things, a change in the energy gap between the two states. This, combined with the allowed values of the shift parameter, will change the constraints on Ω_m.

As mentioned in the BFK paper, in order to have a more complete description of this model, one should also consider adding gravitational and bayonic terms to the dark matter Lagrangian

$$\mathcal{L}_{grav} = -M_{pl}^2(\vec{\nabla}\Phi)^2$$
$$\mathcal{L}_{int} = \alpha\Lambda\frac{\theta}{M_{pl}}\rho_b.$$

In terms of observational sources, the Euclid mission specifically endeavours to study the dark sector. Naturally their observations of the expansion rate of the universe and of weak lensing and baryonic acoustic oscillations will put constraints on dark energy/matter models. One can also determine the expected particle density in galactic halos for this model, which would results in an expected collision rate as observed by dark matter detector, such as the XENON1T experiment.

Appendix A

χ^2 Table

$\Delta\epsilon$	M	χ^2
0.010	0.15916	47.298
0.079	0.15916	47.193
0.147	0.15816	46.930
0.216	0.15616	46.511
0.284	0.15315	45.944
0.353	0.14915	45.240
0.422	0.14515	44.413
0.490	0.14014	43.478
0.559	0.13413	42.452
0.628	0.12713	41.357
0.696	0.12012	40.219
0.765	0.11211	39.063
0.833	0.10310	37.917
0.902	0.09309	36.813
0.971	0.08308	35.784
1.039	0.07207	34.865
1.108	0.06106	34.092
1.177	0.04905	33.504
1.245	0.03704	33.140
1.314	0.02402	33.038
1.382	0.01001	33.239
1.451	-0.00400	33.781
1.520	-0.01802	34.702
1.588	-0.03303	36.040
1.657	-0.04805	37.828
1.726	-0.06406	40.098
1.794	-0.07908	42.876
1.863	-0.09510	46.185
1.931	-0.11211	50.044
2.000	-0.12813	54.461
(ΛCDM)	0.00000	33.653

Table A.1: Best-fit M parameters with associated χ^2 values for various $\Delta\epsilon$ and ΛCDM. The cut-off χ^2 value for $p < .05$ with 30 d.o.f. is 43.773.

Bibliography

[1] Planck Collaboration *et al.*, "Planck 2018 results. VI. Cosmological parameters," *AAP*, vol. 641, p. A6, Sept. 2020. [ADS] [arXiv:1807.06209 [astro-ph.CO]]. See Chapter 3 in particular.

[2] G. Bertone, D. Hooper, and J. Silk, "Particle dark matter: evidence, candidates and constraints," *Phys. Rep.*, vol. 405, pp. 279–390, Jan. 2005. [ADS] [arXiv:hep-ph/0404175].

[3] S. S. McGaugh, J. M. Schombert, G. D. Bothun, and W. J. G. de Blok, "The Baryonic Tully-Fisher Relation," *Astrophys. J. Lett.*, vol. 533, pp. L99–L102, Apr. 2000. [ADS] [arXiv:astro-ph/0003001].

[4] M. Boylan-Kolchin, J. S. Bullock, and M. Kaplinghat, "Too big to fail? The puzzling darkness of massive Milky Way subhaloes," *Mon. Not. R. Astron. Soc.*, vol. 415, pp. L40–L44, July 2011. [ADS] [arXiv:1103.0007 [astro-ph.CO]].

[5] R. A. Flores and J. R. Primack, "Observational and Theoretical Constraints on Singular Dark Matter Halos," *Astrophys. J.*, vol. 427, p. L1, May 1994. [ADS] [arXiv:astro-ph/9402004].

[6] P. Bull *et al.*, "Beyond Λ CDM: Problems, solutions, and the road ahead," *Physics of the Dark Universe*, vol. 12, pp. 56–99, June 2016. [ADS] [arXiv:1512.05356 [astro-ph.CO]] See Section 4.2 for a discussion of small-scale problems.

[7] V. Sahni, "The cosmological constant problem and quintessence," *Classical and Quantum Gravity*, vol. 19, pp. 3435–3448, July 2002. [ADS] [arXiv:astro-ph/0202076].

[8] M. Milgrom, "A modification of the Newtonian dynamics as a possible alternative to the hidden mass hypothesis.," *APJ*, vol. 270, pp. 365–370, Jul 1983. [ADS].

[9] E. G. M. Ferreira, G. Franzmann, J. Khoury, and R. Brandenberger, "Unified superfluid dark sector," *JCAP*, vol. 2019, p. 027, Aug 2019. [ADS] [arXiv:1810.09474 [astro-ph.CO]].

[10] A. G. Riess *et al.*, "Observational Evidence from Supernovae for an Accelerating Universe and a Cosmological Constant," *Astrophys. J.*, vol. 116, pp. 1009–1038, Sept. 1998. [ADS] [arXiv:astro-ph/9805201].

[11] S. Weinberg, *Cosmology*. New York: Oxford University Press Inc., 2008.

[12] T. F. Jordan, "Cosmology calculations almost without general relativity," *American Journal of Physics*, vol. 73, pp. 653–662, July 2005. [ADS] [arXiv:astro-ph/0309756].

[13] S. M. Carroll, "The Cosmological Constant," *Living Rev. Relativ.*, vol. 4, p. 1, Feb. 2001. [ADS] [arXiv:astro-ph/0004075]. We specifically make reference to Chapter 4: *Physics Issues*.

[14] S. M. Carroll, *Spacetime and geometry: an introduction to general relativity*. Noida: Pearson India Education Services Pvt. Ltd., 1st ed., 2016.

[15] T. P. Sotiriou and V. Faraoni, "$f(r)$ theories of gravity," *Rev. Mod. Phys.*, vol. 82, pp. 451–497, Mar 2010. [ADS] [arXiv:0805.1726 [gr-qc]].

[16] M. H. Anderson, J. R. Ensher, M. R. Matthews, C. E. Wieman, and E. A. Cornell, "Observation of bose-einstein condensation in a dilute atomic vapor," *Science*, vol. 269, pp. 198–201, July 1995. [ADS].

[17] R. Baierlein, "The elusive chemical potential," *American Journal of Physics*, vol. 69, pp. 423–434, Apr. 2001. [ADS].

[18] C. J. Pethick and H. Smith, *Bose-Einstein condensation in dilute gases*. Cambridge University Press, 2nd ed., 2008.

[19] P. Kapitza, "Viscosity of liquid helium below the λ-point," *Nature*, vol. 141, p. 74, 1938. [ADS].

[20] J. F. Allen and A. D. Misener, "Flow phenomena in liquid helium ii," *Nature*, vol. 142, pp. 643–644, 1938. [ADS].

[21] M. R. Andrews, C. G. Townsend, H.-J. Miesner, D. S. Durfee, D. M. Kurn, and W. Ketterle, "Observation of interference between two bose condensates," *Science*, vol. 275, pp. 637–641, 1997. [Journal] doi: 10.1126/science.275.5300.637.

[22] A. J. Beekman, L. Rademaker, and J. van Wezel, "An Introduction to Spontaneous Symmetry Breaking," *arXiv e-prints*, p. arXiv:1909.01820, Sept. 2019. [ADS] [arXiv:1909.01820 [hep-th]].

[23] R. C. James, *Mathematics Dictionary*. Chapman & Hall, 5th ed., 1992.

[24] L. Berezhiani, B. Famaey, and J. Khoury, "Phenomenological consequences of superfluid dark matter with baryon-phonon coupling," *JCAP*, vol. 2018, p. 021, Sept. 2018. [ADS] [arXiv:1711.05748 [astro-ph.CO]].

[25] T. Zibold, E. Nicklas, C. Gross, and M. K. Oberthaler, "Classical bifurcation at the transition from rabi to josephson dynamics," *Phys. Rev. Lett.*, vol. 105, p. 204101, Nov 2010. [ADS] [arXiv:1008.3057 [cond-mat.quant-gas]].

[26] R. J. Ballagh, K. Burnett, and T. F. Scott, "Theory of an output coupler for bose-einstein condensed atoms," *Phys. Rev. Lett.*, vol. 78, pp. 1607–1611, Mar 1997. [ADS].

[27] A. J. Leggett, "Bose-einstein condensation in the alkali gases: Some fundamental concepts," *Rev. Mod. Phys.*, vol. 73, pp. 307–356, Apr 2001. [ADS] See page 341 for the differences between the "Rabi", "Josephson", and "Fock" regimes in BEC systems.

[28] M. Betoule *et al.*, "Improved cosmological constraints from a joint analysis of the SDSS-II and SNLS supernova samples," *AAP*, vol. 568, p. A22, Aug. 2014. [ADS] [arXiv:1401.4064 [astro-ph.CO]].

[29] E. S. Pearson and H. O. Hartley, *Biometrika Table for Statisticians*, vol. 1. Cambridge: Cambridge University Press, 1st ed., 1954.

[30] Ø. Elgarøy and T. Multamäki, "On using the cosmic microwave background shift parameter in tests of models of dark energy," *AAP*, vol. 471, pp. 65–70, Aug. 2007. [ADS] [arXiv:astro-ph/0702343].